Mechanical Buckling of FG Saturated Porous Rectangular Plate with Piezoelectric Actuators

M. Jabbari[*]
Associate Professor

M. Rezaei[†]
MSc.

A. Mojahedin[‡]
MSc.

In this study buckling analysis of solid rectangular plate made of porous material bounded with the layers of piezoelectric actuators in undrained condition is investigated. Porous material properties vary through the thickness of plate with a specific function. Distributing of the pores through the plate thickness is assumed to be the nonlinear nonsymmetric distribution. The general mechanical non-linear equilibrium and linear stability equations are derived using the variational formulations to obtain the governing equations of piezoelectric porous plate. The effects of piezoelectric layers on critical buckling load of plate, piezoelectric layer-to-porous plate thickness ratio and actuator voltage are studied. Also, effect of fluid compressibility and variation of porosity on critical buckling load are investigated in the undrained condition. Closed-form solutions is used to derive the critical buckling loads of the plate subjected to mechanical loading. The results obtained for porous plates with the layers of piezoelectric actuators are verified with the known data in literature.

Keywords: buckling analysis, rectangular plate, functionally graded plate, porous material

1 Introduction

Porous material composed of two elements: the main part of the porous material is solid (Body), liquid or gas is the second part. Deflection and buckling problems of the porous plates have been expanded by many authors. Biot [1] described the buckling of a fluid-saturated porous slab under axial compression. He investigated interaction between the pore compressibility effect and critical buckling load. Buckling of porous beams with varying properties were presented by Magnucki and Stasiewicz [2]. Shear deformation theory applied to determine the critical load. They investigated the effect of porosity on buckling load of the beam. The bending and buckling of rectangular plate made of foam material which have nonlinear mechanical properties in thickness direction with its material properties being non-symmetric with respect to middle of the plate were studied by Magnucki et al. [3] They showed the result for a porous/nonlinear symmetric distribution plate.

---

[*] Corresponding Author, Associate Professor, Department of Mechanical Engineering, South Tehran Branch, Islamic Azad University, Tehran, Iran Mohsen.jabbari@gmail.com

[†] MSc., Department of Mechanical Engineering, South Tehran Branch, Islamic Azad University, Tehran, Iran Masoud.rezaey@yahoo.com

[‡] MSc., Department of Mechanical Engineering, South Tehran Branch, Islamic Azad University, Tehran, Iran mojahedin.arvin@gmail.com

The critical buckling load for rectangular plate made of foam with two layers of perfect material was described by Magnucka-Blandzi [4]. The core was made of a metal foam with properties varying across the thickness. The analytical, numerical, and experimental critical buckling load for plate and beam made of foam with two layers of perfect material were studied by Jasion et al. [5]. They obtained global and local buckling-wrinkling of the face sheets of sandwich beams and sandwich circular plates. The values of the critical load compared by the analytical, numerical (FEM), and experimental methods. The poroelastic and thermoelastic coupling parameters for a linear poroelastic saturated rock were investigated by Zimmerman [6]. He deduced that poroelastic coupling parameter is more effective than the thermoelastic parameters. The effects of temperature

gradients on pore pressure and stress distribution by using a non-isothermal poroelasticity theory was described by Ghassemi et al. [7]. Thereafter, the influence of cooling on pore pressure and stresses distribution by displacement discontinuity method was studied by Ghassemi [8]. The poroelastic circular plate under the mechanical loads base on classical plate theory and higher order shear deformation theory, Also thermal forces Base on classical plate theory (CPT) were described by Jabbari et al. [9,10] They investigated the effects of distribution and properties of pores that are saturated by fluid on critical buckling load of plate.

Buckling analysis of porous plates with functional properties have similarities with the FGM plates to some extend. Javaheri et al. [12] presented the buckling of FGM rectangular plates under in-plane mechanical or thermal loads based on the classical and higher order shear deformation plate theories, respectively. the thermal buckling of simply-supported moderately thick rectangular FGM plates based on the FSDT under different types of temperature fields is investigated by Lanhe [13]. Shariat et al. [14] presented a closed-form solution for the buckling analysis of rectangular thick FGM plates based on the TSDT under mechanical and thermal

loads. The buckling analysis of thin FG rectangular plates based on the classical or FSDT under various loads were done by Mohammadi et al. [15], respectively. Bodaghi et al. [16,17] used a Levy-type solution method to investigate the mechanical or thermoelastic buckling of thick FGM rectangular plates based on the TSDT, respectively. Bateni et al. [19]. investigated the effect of temperature dependency of material properties on the critical buckling load. In this study, a four-variable refined plate theory is employed to derive the governing equations of equilibrium. A multi-term Galerkin solution is presented to derive the critical buckling loads/temperatures along with the buckled shape of the plate. Behravan Rad et al. [20] Investigated three-dimensional magneto-elastic analysis of asymmetric variable thickness porous FGM circular plates with non-uniform tractions and Kerr elastic foundations.

A comprehensive review of various analytical and numerical models to predict the bending and buckling under mechanical and thermal loads is done by Swaminathan et al. [21,22]. Chen et al. [23,24] presented the elastic buckling and static bending solutions based on Timoshenko beam theory also free and forced vibrations of shear deformable functionally graded porous beams. One of the techniques exists to increase the buckling load is equipping plates with smart materials. Piezoelectric materials, as sensor and actuator of the most common sub-group of smart materials are used in solid structures to control the deformation, vibration and buckling control of structures. An analytical solution for free vibration analysis of a piezoelectric coupled circular plate with clamped and simply supported boundary conditions based on classical plate theory was showed by Wang et al. [25]. Post-buckling of piezoelectric FGM plates subjected to the thermo-electro-mechanical loading was reported by Liew et al. [26]. They showed a semi-analytical iteration to determine the post-buckling response of the plate. Viliani et al. [27] investigated the active buckling control of smart functionally graded plates using sensor/actuator patches. Closed-form solutions for the critical temperatures of simply supported piezoelectric FGM cylindrical shells based on the higher order displacement field was described Mirzavand and Eslami [28].

They investigated three types of temperature loadings combined with constant applied voltage. Shen [28] presented thermo-electro-mechanical buckling and post-buckling of FGM plates with piezoelectric actuators based on the singular perturbation method.

Thermoelastic buckling analysis of functionally graded circular plates integrated with piezoelectric layers based on the classical plate theory was studied by Khorshidvand et al. [28]. Jabbari et al. [28] considered the stability of sandwich plate with piezoelectric layers and poroelastic core under uniform thermal and electrical field. Also, they achieved their results based on the classical plate theory and first-order theory. They explored the effects of mechanical and thermal properties on stability of poroelastic plate too. Mojahedin et al. [28] studied the buckling of poroelastic plate with piezoelectric layers under electrical, thermal, and mechanical forces. Jabbari et al. [28] considered the buckling of circular porous plate under transverse magnetic field. They explained the effects of mechanical and magnetic properties on stability of porous-magnetic plate.

The purpose of this paper is analyses of rectangular plate made of saturated porous with variety of property along the thickness and is supported by two layers of piezoelectric. The equilibrium and stability equations are derived by Euler equations from the variations that based on the classical plate theory. Close form solution is used to solve the obtained equations with simply supported edges. Also, the effects of pores properties in critical buckling load and stability of plate are investigated. These properties changes with fluid property that is stuck in pores and pore distribution along the thickness.

2 Governing equations

Consider a rectangular plate made of porous materials with length a, and width b, and thickness h, in the middle with two identical piezoelectric layers with thicknesses h_a bounded to its upper and lower surfaces referred to the rectangular Cartesian coordinates (x, y, z), as shown in figure (1).

The material properties are assumed to vary through the thickness according to the following power law distribution. The functional relationship between E and G with z for plate is assume as (Magnucki et al. [2] and Magnucka-Blandzi [4])

$$G(z) = G_0 \left[1 - e_1 \cos \left(\left(\frac{\pi}{2h} \right) \left(z + \frac{h}{2} \right) \right) \right]$$

$$E(z) = E_0 \left[1 - e_1 \cos \left(\left(\frac{\pi}{2h} \right) \left(z + \frac{h}{2} \right) \right) \right] \tag{1}$$

$$e_1 = 1 - \frac{G_1}{G_0} = 1 - \frac{E_1}{E_0}$$

where e_1 is the coefficient of plate porosity $0 < e_1 < 1$, E_1 and E_0 are Young's modulus of elasticity at $z = -h/2$ and $z = h/2$, respectively, $(E_0 \geq E_1)$ and G_1 and G_0 are the shear modulus at $z = -h/2$ and $z = h/2$, respectively, $(G_0 \geq G_1)$. The relationship between the modulus of elasticity and shear modulus of elasticity for $j = 0$ and 1 is $E_j = 2G_j(1 + v)$ where v is Poisson's ratio, which is assumed to be constant across the plate thickness.
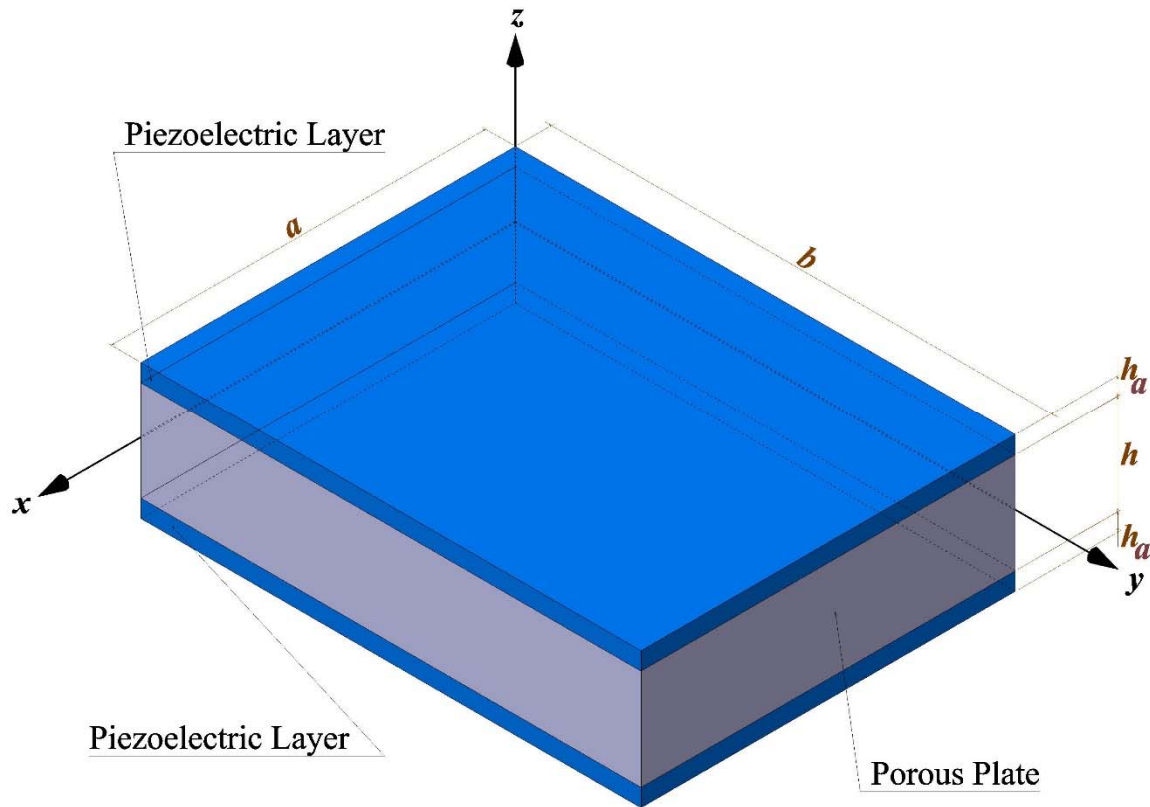
Figure 1 Coordinate system and geometry of a piezoelectric coupled rectangular porous material plate

2.1 Basic equations

The non-linear strain-displacement relations according to the von-Karman assumption are by Brush and Almroth [37]

$$\varepsilon_{xx} = u_{,x} + \frac{1}{2}\left(w_{,x}\right)^2$$
$$\varepsilon_{yy} = v_{,y} + \frac{1}{2}\left(w_{,y}\right)^2 \tag{2}$$
$$\gamma_{xy} = u_{,y} + v_{,x} + w_{,y}w_{,x}$$

Here, ε_{xx} and ε_{yy} are the normal strains and γ_{xy} is the shear strain, where u, v, and w denote the displacement components in the x, y, and z directions, respectively, and comma indicates the partial derivative with respect to its afterwards. Note that transverse shear strains are zero as $\gamma_{yz} = \gamma_{xz} = 0$ in the Kirchhoff plate theory.

The displacement field for the Kirchhoff plate theory is by Wang et al. [38]

$$u(x,y,z) = u_0(x,y) - zw_{0,x}$$
$$v(x,y,z) = v_0(x,y) - zw_{0,y} \tag{3}$$
$$w(x,y,z) = w_0(x,y)$$

Where (u_0, v_0, w_0) represent the displacement on middle plate surface $(z = 0)$.
The linear poroelasticity theory of the Biot has two features by Detournay and Cheng [39]

1. An increase of pore pressure induces a dilation of pore.

2. Compression of the pore causes a rise of pore pressure.

The stress-strain law for the poroelasticity is given by Ghassemi [8] of the plate is written as following:

$$\sigma_{ij}^h = 2G\varepsilon_{ij} + \lambda_u\varepsilon\delta_{ij} - p\alpha\delta_{ij} \tag{4}$$

Where

$$\lambda_u = \frac{2Gv_u}{1 - 2v_u}$$

$$v_u = \frac{v + \alpha B(1 - 2v)/3}{1 - \alpha B(1 - 2v)/3}$$

$$p = M[\zeta - \alpha\varepsilon] \tag{5}$$

$$M = \frac{(2G + 3\lambda)}{3(1 - \alpha B)}B$$

Here, the superscript h is used to denote the porous plate. p is pore fluid pressure, λ_u is the Lame parameters, M is Biot's modulus, ζ is variation of fluid volume content, v_u is undrained Poisson's ratio $v < v_u < 0.5$, B is the skempton coefficient, the pore fluid properties is introduced by the skempton coefficient. The values of the undrained Poisson ratio and the Skempton pore pressure coefficients depend on the pore fluid compressibility. Here, α is the Biot coefficient of effective stress $0 < \alpha < 1$. The Biot coefficient $\left(\alpha = 1 - \frac{G(z)}{G_0}\right)$ indicates the effect of porosity on the solid constituents of poroelastic plate and it shows the effect of generated stresses in the pores on the poroelastic material in undrained condition $(\zeta = 0)$ and $(1 - \alpha B)$ is relation between drained bulk modulus and undrained bulk modulus.
The term αB is coupling between pore fluid effects and macroscopic deformation Zimmerman [6], and ε is the volumetric strain.

The two dimensional stress-strain law for plane-stress condition in the Cartesian coordinate for the undrained condition $(\zeta = 0)$ is given by

$$\begin{aligned}
\sigma_{xx}^h &= A_1(z)\varepsilon_{xx} + B_1(z)\varepsilon_{yy} \\
\sigma_{yy}^h &= A_1(z)\varepsilon_{yy} + B_1(z)\varepsilon_{xx} \\
\sigma_{xy}^h &= G(z)\gamma_{xy}
\end{aligned} \tag{6}$$

By substituting the third and fourth equations of (5) into Eq. (4), terms $A_1(z), B_1(z), C_1(z)$ and $R_1(z)$ become

$$\begin{aligned}
A_1(z) &= 2G(z) + (\lambda_u + M\alpha^2)R(z) \\
B_1(z) &= (\lambda_u + M\alpha^2)R(z)
\end{aligned}$$

$$R(z) = 1 - \frac{\lambda_u + M\alpha^2}{2G(z) + \lambda_u + M\alpha^2} \tag{7}$$

The stress-strain law for piezoelectric parts by Liew et al. [27] of the plate are written as following:

$$\{\sigma\}^p = \begin{Bmatrix} \sigma_{xx}^p \\ \sigma_{yy}^p \\ \sigma_{xy}^p \end{Bmatrix} = \begin{bmatrix} c_{11} & c_{12} & 0 \\ c_{12} & c_{22} & 0 \\ 0 & 0 & c_{66} \end{bmatrix} \begin{Bmatrix} \varepsilon_{xx}^p \\ \varepsilon_{yy}^p \\ \varepsilon_{xy}^p \end{Bmatrix} - \begin{bmatrix} 0 & 0 & e_{31} \\ 0 & 0 & e_{32} \\ 0 & 0 & 0 \end{bmatrix} \begin{Bmatrix} E_x \\ E_y \\ E_z \end{Bmatrix} \tag{8}$$

Where the superscript p is used to denote the piezoelectric layer, c_{ij} $(i, j = 1,2,6)$ is the elastic stiffness of the layers given by

$$c_{11} = c_{22} = \frac{2G}{(1-v)}$$
$$c_{12} = c_{21} = \frac{2Gv}{(1-v)} \tag{9}$$
$$c_{66} = G$$

The piezoelectric stiffness e_{31} and e_{32} can be expressed in terms of the dielectric constants d_{31} and d_{32}. The elastic stiffness c_{ij} $(i, j = 1,2,6)$ of the piezoelectric actuator layers as

$$e_{31} = (d_{31}c_{11} + d_{32}c_{21})$$
$$e_{32} = (d_{31}c_{12} + d_{32}c_{22}) \tag{10}$$

As only the transverse electric field component E_z is dominant in the plate type piezoelectric material, it is assumed that

$$\begin{Bmatrix} E_x \\ E_y \\ E_z \end{Bmatrix} = \begin{Bmatrix} 0 \\ 0 \\ V_a/h_a \end{Bmatrix} \tag{11}$$

Where V_a is the voltage applied to the actuators in the thickness direction.

2.2 Strain energy

The total virtual potential energy of the plate as the sum of total virtual strain energy and virtual potential energy of the applied loads is equal to

$$\delta U^h = \frac{1}{2} \int_0^a \int_0^b \int_{-h/2}^{+h/2} (\sigma_{xx}^h \delta\varepsilon_{xx} + \sigma_{yy}^h \delta\varepsilon_{yy} + \sigma_{xy}^h \delta\gamma_{xy})dxdydz \tag{12}$$

$$\delta U^p = \frac{1}{2} \int_0^a \int_0^b \int_{-h/2-h_a}^{-h/2} (\sigma_{xx}^p \delta\varepsilon_{xx} + \sigma_{yy}^p \delta\varepsilon_{yy} + \sigma_{xy}^p \delta\gamma_{xy} - E_z \delta D_z)dxdydz$$
$$+ \frac{1}{2} \int_0^a \int_0^b \int_{h/2}^{h/2+h_a} (\sigma_{xx}^p \delta\varepsilon_{xx} + \sigma_{yy}^p \delta\varepsilon_{yy} + \sigma_{xy}^p \delta\gamma_{xy} - E_z \delta D_z)dxdydz \tag{13}$$

$$\delta V = \delta U^p + \delta U^h \tag{14}$$

Substituting the strain-displacement relations from Eqs. (2) and Eq. (3) into Eq. (14), and apply the Green-Gauss theorem to relieve the virtual displacements, result in the following three equilibrium equations by Eslami [40]

$$\delta u_0 : \ N_{xx,x} + N_{xy,y} = 0$$
$$\delta v_0 : \ N_{xy,x} + N_{yy,y} = 0 \tag{15}$$
$$\delta w_0 : \ M_{xx,xx} + M_{yy,yy} + 2M_{xy,xy} + N_{xx}w_{0,xx} + N_{yy}w_{0,yy} + 2N_{xy}w_{0,xy} = 0$$

Where N_{ij} and M_{ij} are the force and moment resultants defined by

$$\left(N_{ij}, M_{ij}\right) = \int_{-h/2-h_a}^{-h/2}(1,z)\sigma_{ij}^a dz + \int_{-h/2}^{h/2}(1,z)\sigma_{ij}dz + \int_{h/2}^{h/2+h_a}(1,z)\sigma_{ij}^a dz \quad ij = xx, yy, xy \tag{16}$$

3 Stability equations

Consider an equilibrium position described by displacement components u_0^0, v_0^0, and w_0^0. Each of these components is perturbed from the primary equilibrium state. An equilibrium state exists adjacent to the primary one, described by the displacement components as by Eslami [40]

$$u_0 \rightarrow u_0^0 + u_0^1$$
$$v_0 \rightarrow v_0^0 + v_0^1 \tag{17}$$
$$w_0 \rightarrow w_0^0 + w_0^1$$

Here, a superscript 1 indicates the magnitude of increment (perturbation). Accordingly, the stress resultants are divided into two terms representing the stable equilibrium and the neighboring state. The stress resultants with superscript 1 are linear functions of displacement with superscript 1. Considering this and using Eqs. (15) and Eqs. (17), the stability equations become

$$\delta u_0^1 : \ N_{xx,x}^1 + N_{xy,y}^1 = 0 \tag{18}$$
$$\delta v_0^1 : \ N_{xy,x}^1 + N_{yy,y}^1 = 0$$
$$\delta w_0^1 : \ M_{xx,xx}^1 + M_{yy,yy}^1 + 2M_{xy,xy}^1 + N_{xx}^0 w_{0,xx}^1 + N_{yy}^0 w_{0,yy}^1 + 2N_{xy}^0 w_{0,xy}^1 = 0$$

The stability equations in terms of the displacement components may be obtained by inserting Eqs. (16) into the above equations. Upon substitution, second and higher order terms of the incremental displacements may be omitted. Resulting equations are three stability equations based on the Kirchhoff plate theory for porous material plate.

$$A_2^* u_{0,xx}^1 + C_2^* u_{0,yy}^1 + (B_2^* + C_2^*)v_{0,xy}^1 - \left(A_3 w_{0,xxx}^1 + (B_3 + 2C_3)w_{0,xyy}^1\right) = 0$$
$$(B_2^* + C_2^*)u_{0,xy}^1 + A_2^* v_{0,yy}^1 + C_2^* v_{0,xx}^1 - \left(A_3 w_{0,yyy}^1 + (B_3 + 2C_3)w_{0,xxy}^1\right) = 0 \tag{19}$$
$$-\left(A_3 u_{0,xxx}^1 + (B_3 + 2C_3)u_{0,xyy}^1\right) - \left(A_3 v_{0,yyy}^1 + (B_3 + 2C_3)v_{0,xxy}^1\right)$$
$$+ \left(A_4^*\left(w_{0,xxxx}^1 + w_{0,yyyy}^1\right) + 2(B_4^* + 2C_4^*)w_{0,xxyy}^1\right) + N_{xx}^0 w_{0,xx}^1$$
$$+ N_{yy}^0 w_{0,yy}^1 = 0$$

Where

$$A_2, A_3, A_4 = \int_{-h/2}^{+h/2} A_1(z)(1, z, z^2)dz$$

$$B_2, B_3, B_4 = \int_{-h/2}^{+h/2} B_1(z)(1, z, z^2)dz$$

$$C_2, C_3, C_4 = \int_{-h/2}^{+h/2} G(z)(1, z, z^2)dz$$

$$A_2^* = A_2 + 2h_a c_{11}, \qquad A_4^* = A_4 + \left(hh_a^2 + \frac{1}{2}h^2 h_a + \frac{2}{3}h_a^3\right)c_{11}$$

$$B_2^* = B_2 + 2h_a c_{12}, \qquad B_4^* = B_4 + \left(hh_a^2 + \frac{1}{2}h^2 h_a + \frac{2}{3}h_a^3\right)c_{12}$$

$$C_2^* = C_2 + 2h_a c_{66}, \qquad C_4^* = C_4 + \left(hh_a^2 + \frac{1}{2}h^2 h_a + \frac{2}{3}h_a^3\right)c_{66}$$

(20)

4 Boundary conditions

As stated, only plates with all edges simply supported are consider in this work, Out-of-plane boundary conditions for simply supported edges are

$$x = 0, a : \ w_0^1 = M_{xx}^1 = 0$$
$$y = 0, b : \ w_0^1 = M_{yy}^1 = 0$$

(21)

The in-plane boundary conditions of the simply supported edges may be of the free to move (FM) type. This is classified as follow

$$x = 0, a :$$

$$u_o^1 = finite, \ v_o^1 = finite, \qquad N_{xy}^0 = 0, \qquad N_{xx}^0 = -\frac{P_x}{b} \ (FM)$$

(22)

$$y = 0, b :$$

$$u_o^1 = finite, \ v_o^1 = finite, \qquad N_{xy}^0 = 0, \qquad N_{yy}^0 = -\frac{P_x}{b} - 2V_a(d_{31}c_{12} + d_{23}c_{22}) \ (FM)$$

Where a bar over each parameter stands for the known external forces applied at boundaries.

5 Mechanical buckling analysis

The functions for displacements that satisfy the governing equations and boundary conditions are

$$u_o^1 = \sum_{m=1}^{M} \sum_{n=1}^{N} u_{mn}^1 \cos(\beta x) \sin(\gamma y)$$

(23)

$$v_o^1 = \sum_{m=1}^{M} \sum_{n=1}^{N} v_{mn}^1 \sin(\beta x) \cos(\gamma y)$$

$$w_0^1 = \sum_{m=1}^{M} \sum_{n=1}^{N} w_{mn}^1 \sin(\beta x) \sin(\gamma y)$$

Where

$$\beta = \frac{m\pi}{a}, \quad \gamma = \frac{n\pi}{b} \qquad m, n = 1, 2, 3, \ldots$$

Substitution of Eqs. (23) into Eqs. (19) yield

$$
\begin{aligned}
K_{11}^* &= A_2^* \beta^2 + C_2^* \gamma^2 \\
K_{12}^* &= \beta\gamma(B_2^* + C_2^*) \\
K_{13} &= -\left(A_3\beta^3 + \beta\gamma^2(B_3 + 2C_3)\right) \\
K_{22}^* &= A_2^*\gamma^2 + C_2^*\beta^2 \\
K_{23} &= -\left(A_3\gamma^3 + \beta^2\gamma(B_3 + 2C_3)\right) \\
K_{33}^* &= A_4^*(\beta^4 + \gamma^4) + 2\beta^2\gamma^2(B_4^* + 2C_4^*) + N_{xx}^0\beta^2 + N_{yy}^0\gamma^2
\end{aligned}
\tag{24}
$$

For a nontrivial solution of these equations, the coefficients of functions must be set to zero. Setting $|K_{ij}| = 0$, the value of the N_{xx}^0 is found as

$$-N_{xx}^0\beta^2 - N_{yy}^0\gamma^2 = \frac{P_1^*}{P_2^*} + A_4^*(\beta^4 + \gamma^4) + 2\beta^2\gamma^2(B_4^* + 2C_4^*) \tag{25}$$

Where

$$
\begin{aligned}
P_1^* &= K_{11}^* K_{23}^2 - 2K_{12}^* K_{23} K_{13} + K_{22}^* K_{13}^2 \\
P_2^* &= K_{11}^* K_{22}^* - (K_{12}^*)^2
\end{aligned}
$$

By substitution ($m = 1, n = 1$), the critical mechanical load for porous-elastic plate buckling is obtained. Introducing the dimensionless form for P_x as $P^* = \frac{P_x}{G_0 h^2}$ and substitution of Eqs. (22) into Eq. (25) and solving for P^* yields

$$
\begin{aligned}
P^* = \frac{b}{G_0(\beta^2 + \gamma^2)h^2} &\left[\frac{P_1^*}{P_2^*} + A_4^*(\beta^4 + \gamma^4) + 2\beta^2\gamma^2(B_4^* + 2C_4^*) \right. \\
&\left. - 2\gamma^2 V_a(d_{31}c_{12} + d_{23}c_{22}) \right]
\end{aligned}
\tag{26}
$$

6   Result and discussion

The buckling of rectangular plates made of porous material with variable properties along the thickness with piezoelectric layers under uniform outside compressive load is investigated in this paper. The effects of poroelastic and piezoelectric layers parameters on critical buckling load P^* are investigated and presented.

Poisson's ratio v for porous plate and piezoelectric layers are equal, also we consider G shear modulus of piezoelectric layers equal to G_0. Piezoelectric constants d_{31}, d_{32} are 2.54×10^{-10} m/V .

The variation of the critical buckling load versus the plate aspect ratio for three various voltage actuators are shown in figure (2). It is apparent from this figure that the P^* can be increased by applying a negative voltage on the actuator layers, and the effect of V_a becomes more significant at higher plate aspect ratios.
The effect of dimension changes on the critical buckling load of the porous/nonlinear nonsymmetric distribution plate. By increasing the length to width ratio of the plate, the critical buckling load P^* reduces.

Figure (2) shows the critical buckling load for porous plate subjected to various actuator voltages by increasing the thickness of porous plate. As seen in these figure, by increasing the thickness of porous part, effect of voltage decreases.

Figure (3) shows the effect of the ratio of the piezoelectric layer thickness on the critical buckling load subjected to various actuator voltages is presented. It is seen that with an increase in the piezo thickness to width ratio, the P^* increases. Also by increasing voltage from -500 to 500 the critical buckling load decreases.

Figure (4) shows the effect of porous and various actuator voltages on the critical buckling load for porous/nonlinear symmetric distribution plates. It is seen that by increasing the porosity of the plate, the critical buckling load P^* decreases. Also with an increase the voltage the P^* decreases.

Figures (5) shows the effect of porous and piezo thickness on the critical buckling load for the porous/nonlinear nonsymmetric distribution plate. As seen in these figure, by increasing the thickness of piezo layer, the critical buckling load P^* increases. By increasing the porosity, the free spaces within the plate increases and shear modulus decrease with respect to the first of Eqs. (1). Also, increasing the porosity of the plate decreases the critical buckling load.

In Figure (6) the effect of pores distribution on critical buckling load for the undrained condition and for simply supported edges is presented. It is observed that the pores distribution and e_1 have significant effect on the critical buckling load. In this figure it is seen that by increasing porosity the buckling load decreases. Also it can be seen that for the plate with high porosity, adding the piezo layer has better effect on stability of the plate with constant thickness of the porous plate.

In investigation of porous materials, properties of pores is so important in order to, in express of behavior of porous plate, it is seperated into drained and undrained conditions. In undrained condition, compressibility of fluid that is struck in pores are illustrated by Skempton coefficient (see Eq. (5)) that change between 0 and 1. As long as the compressibility of fluid is high, Skempton coefficient is willing to zero which results is just for drained condition. However, by decrease the compressibility Skempton coefficient increase up to 1 that plate behavior about the same as hemogenous plate without pores. As can be shown in figures (7). by increasing Skempton coefficient the critical buckling load P^* of the plate is increased. In addition, the figures show the effect of actuator voltages on the buckling load that by increasing the actuator voltage of the plate, the critical buckling load P^* decreases.

Figure (8) shows the effect of compressibility of the pore and piezo thickness on the critical buckling load for the porous/nonlinear nonsymmetric distribution plate. As seen in these figure, by increasing the thickness of piezo layer, the critical buckling load P^* increases. By decreasing the compressibility of the pore, the critical buckling load decreases.

In figures (9) and (10) the effect of compressibility of the pore on critical buckling load is presented. It is observed that the compressibility of the pore have effect on the critical buckling load. In this figure it is seen that by decreasing compressibility of the pore the buckling load decreases. Also it can be seen that by adding the piezo layer has better effect on stability of the plate with constant thickness of the porous plate.
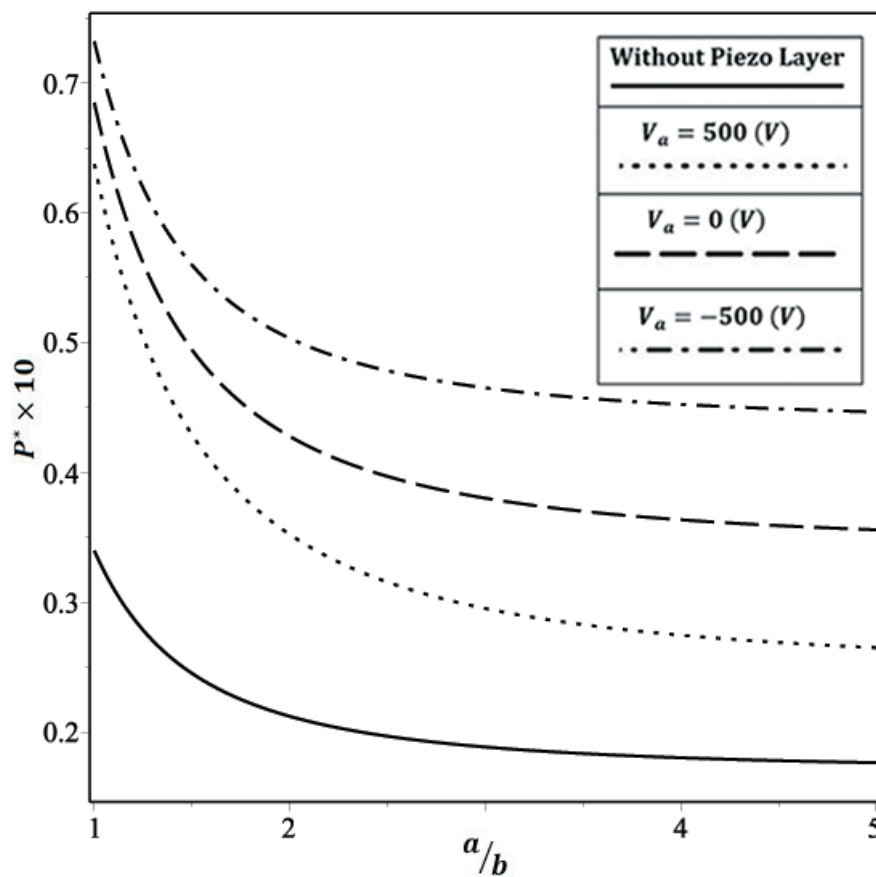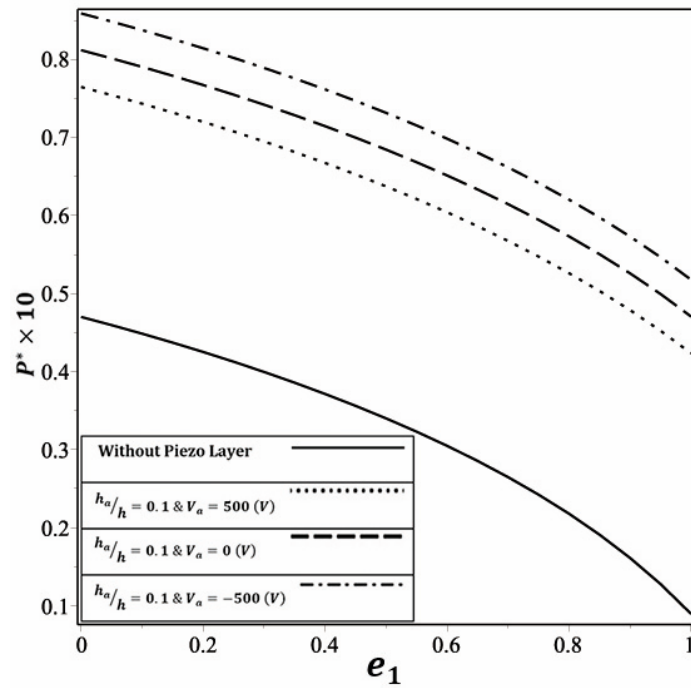

Figure 2 Critical buckling load ($P^* \times 10$) vs. length to width ratio of the porous/nonlinear nonsymmetric distribution plate with piezoelectric layers, for the cases of $[V_a = -500, 0, 500\ V]$, $B = 0.5$, $e_1 = 0.5$ with $\nu = 0.3$, $h_a/h = 0.1$.
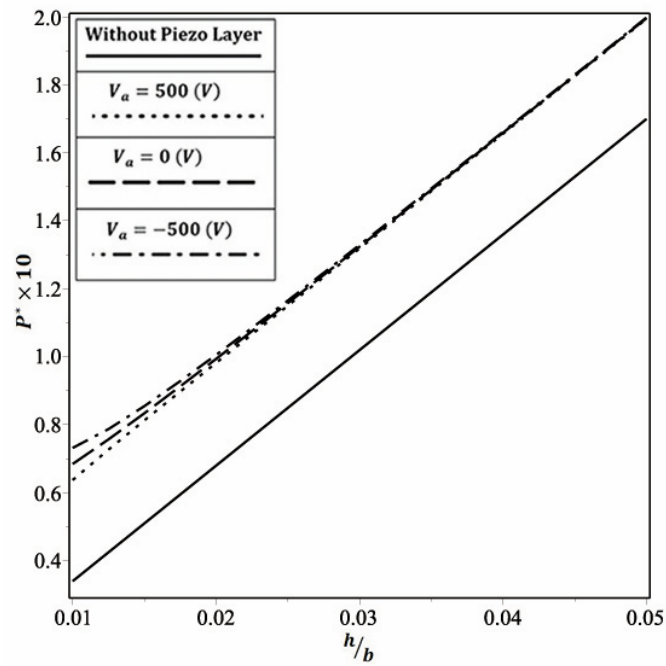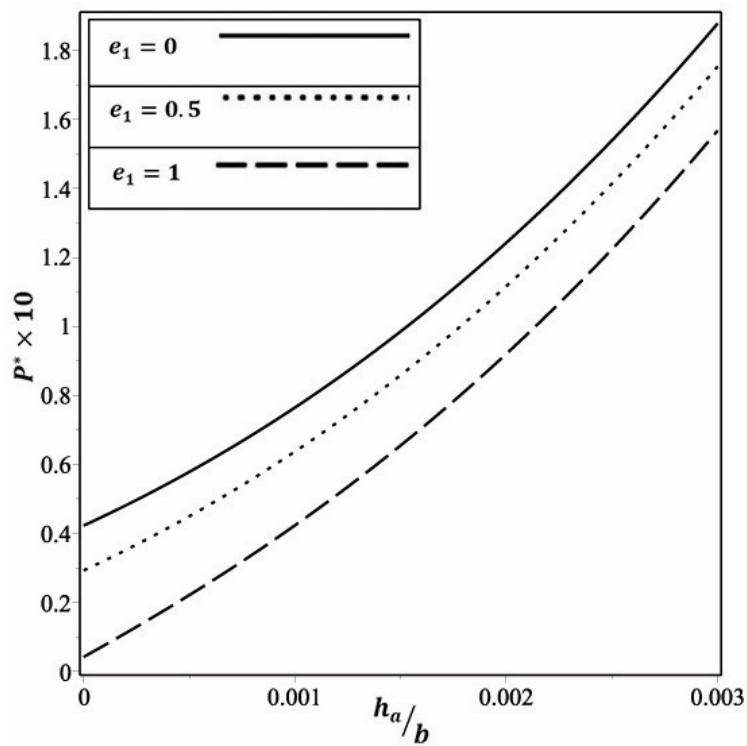
Figure 3 Critical buckling load ($P^* \times 10$) vs. thickness to width ratio of the porous/nonlinear nonsymmetric distribution plate with piezoelectric layers, for the cases of $[V_a = -500, 0, 500\ V]$, $= 0.5$, $e_1 = 0.5$ with $v = 0.3$, $h_a = 0.001$.
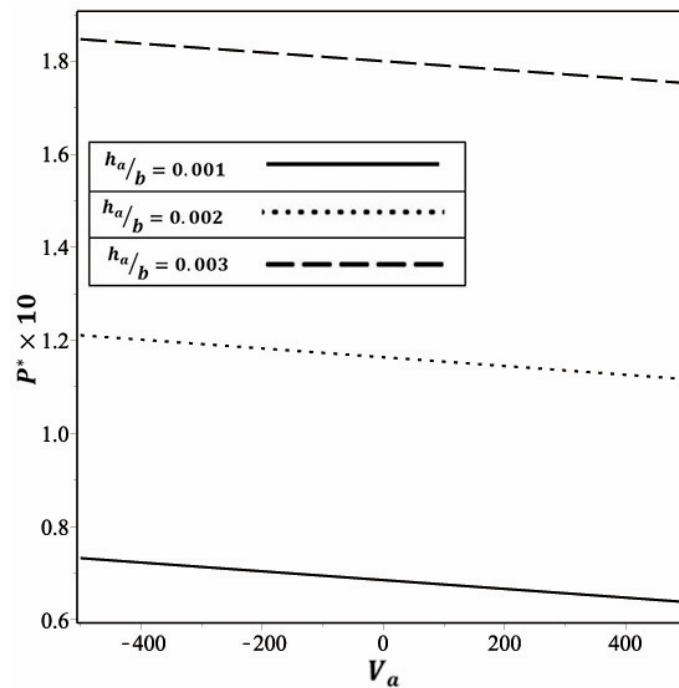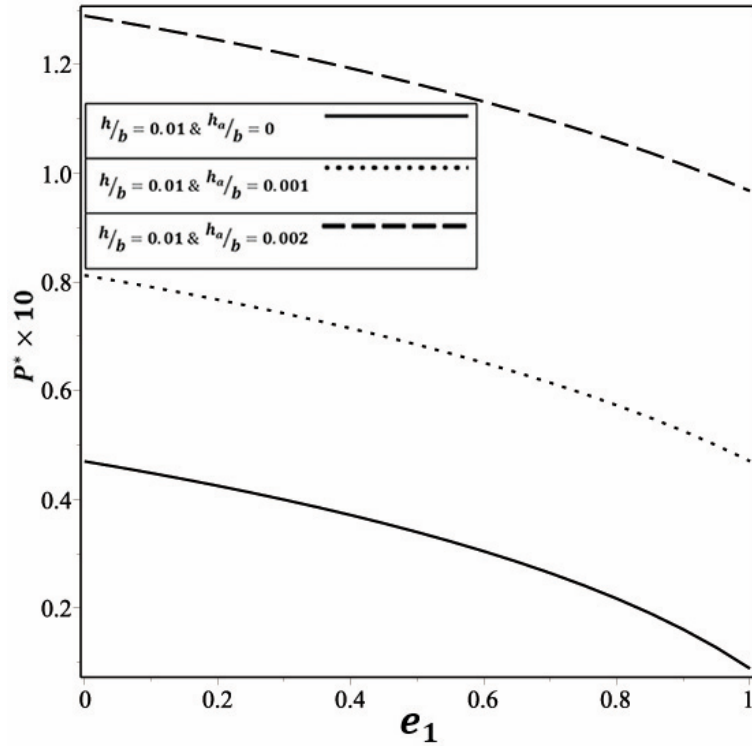

Figure 4 Critical buckling load ($P^* \times 10$) vs. the actuator voltage of the porous/nonlinear nonsymmetric distribution plate with piezoelectric layers, for the cases of $[h_a/b = 0.001, 0.002, 0.003]$, $= 0.5$, $e_1 = 0.5$ with $v = 0.3$.
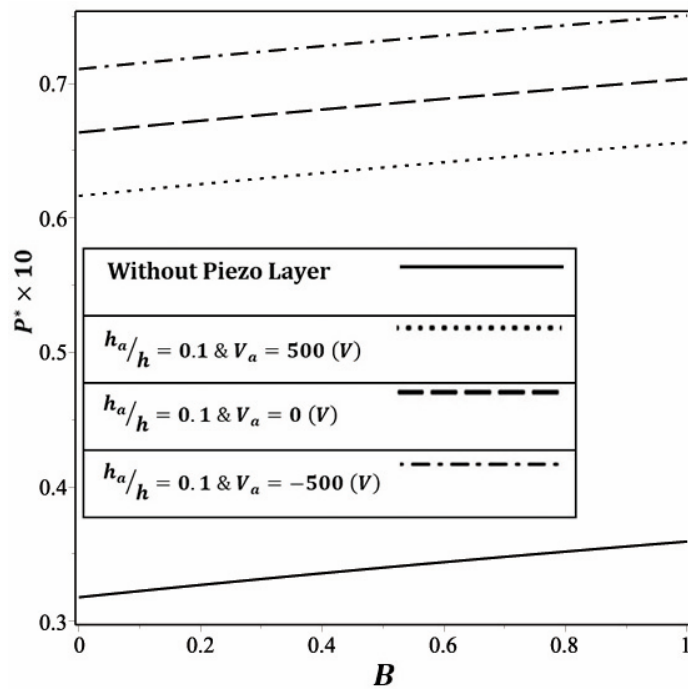
Figure 5 Critical buckling load ($P^* \times 10$) vs. coefficient of porosity of the porous/nonlinear nonsymmetric distribution plate with piezoelectric layers, for the cases of $[V_a = -500, 0, 500\,V]$, $= 0.5$, $[a/b = 1,\ h/b = 0.01, h_a/h = 0.1]$, with $v = 0.3$.
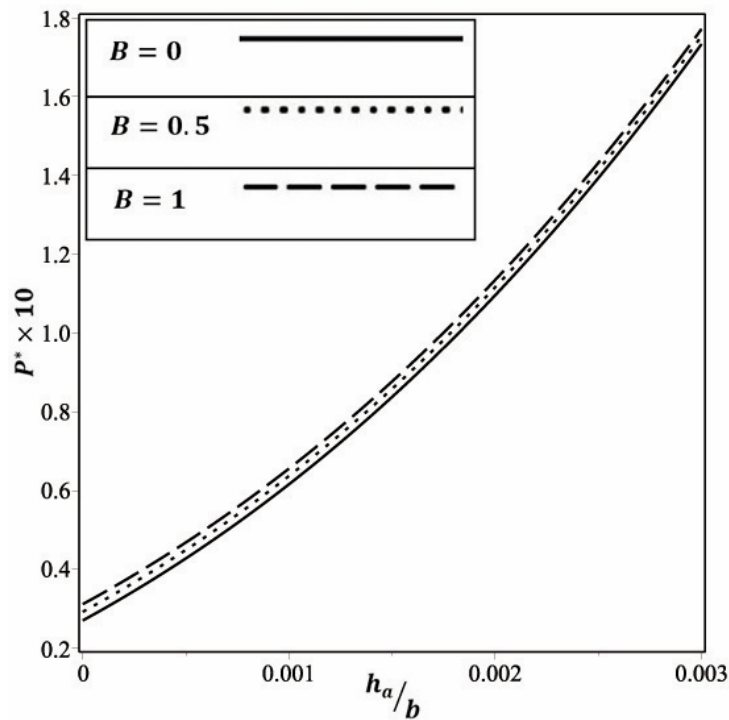

Figure 6 Critical buckling load ($P^* \times 10$) vs. thickness of piezo layer to width of the porous/nonlinear nonsymmetric distribution plate with piezoelectric layers, for the cases of $[e_1 = 0, 0.5, 1]$, $= 0.5$, $[V_a = 500\,V]$, with $[a/b = 1,\ h/b = 0.01]$, $v = 0.3$.
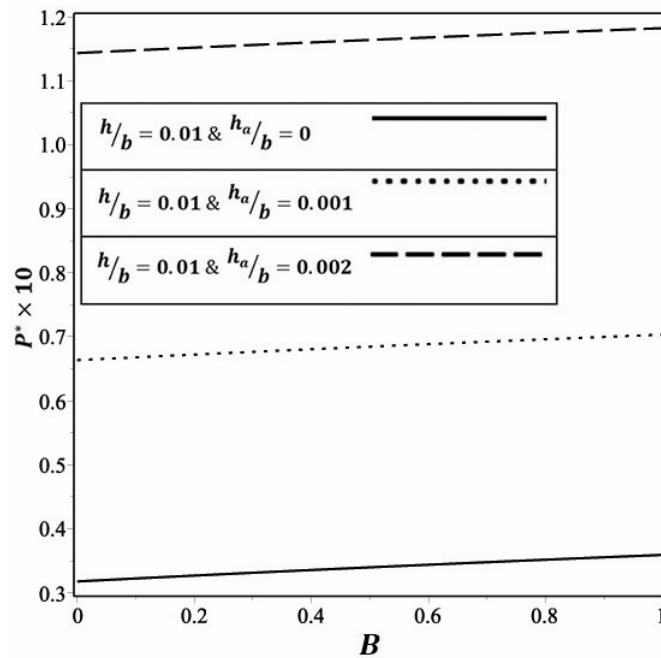
Figure 7 Critical buckling load ($P^* \times 10$) vs. coefficient of porosity of the porous/nonlinear nonsymmetric distribution plate with piezoelectric layers, for the cases of $[h_a/b = 0, 0.001, 0.002]$, $= 0.5$, $[V_a = 0\ V]$, with $[a/b = 1,\ h/b = 0.01]$, $\nu = 0.3$.

Figure 8 Critical buckling load ($P^* \times 10$) vs. the Skempton coefficient of the porous/nonlinear nonsymmetric distribution plate with piezoelectric layers, for the cases of $[V_a = -500, 0, 500\ V]$, $= 0.5$, $[a/b = 1,\ h/b = 0.01, h_a/h = 0.1]$, with $\nu = 0.3$.

Figure 9 Critical buckling load ($P^* \times 10$) vs. the Skempton coefficient of the porous/nonlinear nonsymmetric distribution plate with piezoelectric layers, for the cases of $[B = 0, 0.5, 1]$, $e_1 = 0.5$, $[a/b = 1, \ h/b = 0.01]$, with $v = 0.3$.

Figure 10 Critical buckling load ($P^* \times 10$) vs. the Skempton coefficient of the porous/nonlinear nonsymmetric distribution plate with piezoelectric layers, for the cases of $[h_a/b = 0, 0.001, 0.002]$, $[V_a = 0 \ V]$, $e_1 = 0.5$, $[a/b = 1, \ h/b = 0.01]$, with $v = 0.3$.

7 Conclusions

In the present article, the energy method is used for the buckling analysis of plate made of pore material and derivation is based on the classical plate theory with the assumption that the porosity of the material changes as a specific function. The equilibrium and stability equations for a porous rectangular plate bonded with two piezoelectric layers in upper and lower sides of the plate as a single structural member is obtained. The boundary conditions of plate are assumed to be simply supported. Two edges of the plate is subjected to uniform compressive in-plane loads. The effects of porosity and piezoelectric layers on mechanical buckling capacity of rectangular plates as closed-form solution are presented. It is concluded that:

1. By increasing the coefficient of porosity e_1 the buckling load P^* is reduced.

2. The critical load P^* will increase when the ratios h_a/b, h/b, and h_a/h increase.

3. The application of negative voltage on the actuator layers can improve the mechanical buckling strength, and the critical buckling load can be controlled by applying a suitable voltage on the actuator layers.

4. By increasing the Skempton coefficient, the compressibility of fluid within the pores decrease and the buckling load P^* increases.

Acknowledgements

References

[1] Biot, M.A., "Theory of Buckling of a Porous Slab and its Thermoelastic Analogy", J. Appl. Mech. ASME, Vol. 31, No. 2, pp. 194-198, (1964).

[2] Magnucki, K., and Stasiewicz, P., "Elastic Buckling of a Porous Beam", J. Theor Appl. Mech. Vol. 42, No. 4, pp. 859-868, (2004).

[3] Magnucki, K., Malinowski, M., and Kasprzak, J.," Bending and Buckling of a Rectangular Porous Plate", Steel Compos Struct, Vol. 6, No. 4, pp. 319-333, (2006).

[4] Magnucka-Blandzi, E., "Dynamic Stability of a Metal Foam Circular Plate", J. Theor Appl. Mech. Vol. 47, No. 2, pp. 421-433, (2009).

[5] Jasion, P., Magnucka-Blandzi, E., Szyc, W., and Magnucki, K., "Global and Local Buckling of Sandwich Circular and Beam-rectangular Plates with Metal Foam Core", Thin-Walled Struct, Vol. 61, pp. 154-161, (2012).

[6] Zimmerman, R.W., "Coupling in Poroelasticity and Thermoelasticity", Int. J. Rock Mech. Min Sci, Vol. 37, No. 1, pp. 79-87, (2000).

[7] Ghassemi, A., and Zhang, Q., "A Transient Fictitious Stress Boundary Element Method for Poro-thermoelastic Media", J. Eng Analysis with Boundary Elements, Vol. 28, No. 11, pp. 1363-1373, (2004).

[8] Ghassemi, A., "Stress and Pore Pressure Distribution around a Pressurized, Cooled Crack in Low Permeability Rock", Proceedings of the Thirty-Second Workshop on Geothermal Reservoir Engineering, Stanford University, Stanford, California, USA, January, (2007).

[9] Jabbari, M., Mojahedin, A., Khorshidvand, A.R., and Eslami, M.R., "Buckling Analysis of Functionally Graded Thin Circular Plate made of Saturated Porous Materials", ASCE's J. Eng. Mech. Vol. 140, pp. 287-295, (2013).

[10] Mojahedin, A., Jabbari, M., Khorshidvand, A.R., and Eslami, M.R., "Buckling Analysis of Functionally Graded Circular Plates made of Saturated Porous Materials Based on Higher order Shear Deformation Theory", Thin-Walled Struct. Vol. 99, pp. 83–90, (2016).

[11] Jabbari, M., Hashemitaheri, M., and Mojahedin, A., "Thermal Buckling Analysis of Functionally Graded Thin Circular Plate made of Saturated Porous Materials", J. Therm. Stress. Vol. 37, pp. 202-220, (2014).

[12] Javaheri, R., and Eslami, M.R., "Buckling of Functionally Graded Plates under in-plane Compressive Loading", ZAMM, Vol. 82, pp. 277-283, (2002).

[13] Javaheri, R., and Eslami, M.R., "Thermal Buckling of Functionally Graded Plates", AIAA J. Vol. 40, pp. 162-169, (2002).

[14] Javaheri, R., and Eslami, M.R., "Thermal Buckling of Functionally Graded Plates Based on Higher Order Theory", J. Therm. Stress. Vol. 25, No. 7, pp. 603-625, (2002).

[15] Lanhe, W., "Thermal Buckling of a Simply Supported Moderately Thick Rectangular FGM Plate", Compos. Struct. Vol. 64, No. 2, pp. 211-218, (2004).

[16] Shariat, B.A.S., and Eslami, M.R., "Buckling of Thick Functionally Graded Plates under Mechanical and Thermal Loads", Compos. Struct. Vol. 78, No. 3, pp. 433-439, (2007).

[17] Mohammadi, M., Saidi, A.R., and Jomehzadeh, E., "A Novel Analytical Approach for the Buckling Analysis of Moderately Thick Functionally Graded Rectangular Plates with Two Opposite Edges Simply Supported", Mech. Eng. Sci. Vol. 224, pp. 1831-1841, (2010).

[18] Mohammadi, M., Saidi, A.R., and Jomehzadeh, E., "Levy Solution for Buckling Analysis of Functionally Graded Rectangular Plates", Appl. Compos. Mater. Vol. 17, pp. 81-93, (2010).

[19] Bodaghi, M., and Saidi, A.R., "Levy-type Solution for Buckling Analysis of Thick Functionally Graded Rectangular Plates Based on the Higher-order Shear Deformation Plate Theory", Appl. Math. Model. Vol. 34, No. 11, pp. 3659-3673, (2010).

[20] Bodaghi, M., and Saidi, A.R., "Thermoelastic Buckling Behavior of Thick Functionally Graded Rectangular Plates", Arch. Appl. Mech. Vol. 81, No. 11, pp. 1555-1572, (2011).

[21] Bateni, M., Kiani, Y., and Eslami, M.R., "A Comprehensive Study on Stability of FGM Plates", Int. J. Mech. Sci. Vol. 75, pp. 134-144, (2013).

[22] Behravan Rad, A., and Shariyat, M., "Three-dimensional Magneto-elastic Analysis of Asymmetric Variable Thickness Porous FGM Circular Plates with Non-uniform Tractions and Kerr Elastic Foundations", Compos. Struct. Vol. 125, pp. 558-574, (2015).

[23] Swaminathan, K., Naveenkumar, D.T., Zenkour, A.M., and Carrera, E., "Stress, Vibration and Buckling Analyses of FGM Plates-A State-of-the-art Review", Compos. Struct. Vol. 120, pp. 10-31, (2015).

[24] Chen, D., Yang, J., and Kitipornchai, S., "Elastic Buckling and Static Bending of Shear Deformable Functionally Graded Porous Beam", Compos. Struct. Vol. 133, pp. 54–61, (2015).

[25] Chen, D., Yang, J., and Kitipornchai, S., "Free and Forced Vibrations of Shear Deformable Functionally Graded Porous Beams", Int. J. Mech. Sci. Vol. 108-109, pp. 14–22, (2016).

[26] Wang, Q., Quek, S.T., Sun, C.T., and Liu, X., "Analysis of Piezoelectric Coupled Circular Plate", Smart. Mater. Struct. Vol. 10, pp. 229–239, (2001).

[27] Liew, K.M., Yang, J., and Kitipornchai, S., "Postbuckling of Piezoelectric FGM Plates Subject to Thermo-electro-mechanical Loading", Int. J. Solid Struct. Vol. 40, No. 15, 3869–3892, (2003).

[28] Viliani, N.S., Khalili, S.M.R., and Porrostami, H., "Buckling Analysis of FG Plate with Smart Sensor/actuator", J. Solid Mech. Vol. 1, No. 3, pp. 201–212, (2009).

[29] Mirzavand, B., and Eslami, M.R., "Thermal Buckling of Simply Supported Piezoelectric FGM Cylindrical Shells", J. Therm. Stresses, Vol. 30, No. 11, pp. 1117–1135, (2007).

[30] Shen, H.S., "Postbuckling of Shear Deformable Laminated Plates with Piezoelectric Actuators under Complex Loading Conditions", Int. J. Solids Struct. Vol. 38, No. 44–45, pp. 7703–7721, (2001).

[31] Shen, H.S., "Postbuckling of FGM Plates with Piezoelectric Actuators under Thermo-electro-mechanical Loadings", Int. J. Solids Struct. Vol. 42, No. 23, pp. 6101–6121, (2005).

[32] Shen, H.S., and Noda, N., "Postbuckling of Pressure-loaded FGM Hybrid Cylindrical Shells in Thermal Environments", Compos. Struct. Vol. 77, No. 4, pp. 546–560, (2007).

[33] Khorshidvand, A.R., Jabbari, M., and Eslami, M.R., "Thermoelastic Buckling Analysis of Functionally Graded Circular Plates Integrated with Piezoelectric Layers", J. Therm. Stresses, Vol. 35, pp. 695–717, (2012).

[34] Jabbari, M., Farzaneh Joubaneh, E., and Mojahedin, A., "Thermal Buckling Analysis of a Porous Circular Plate with Piezoelectric Actuators Based on First Order Shear Deformation Theory", Int. J. Mech. Sci. Vol. 83, pp. 57-64, (2014).

[35] Farzaneh Joubaneh, E., Mojahedin, A., Khorshidvand, A.R., and Jabbari, M.," Thermal Buckling Analysis of Porous Circular Plate with Piezoelectric Sensor-actuator Layers under Uniform Thermal Load", J. Sandwich Struct. Mater. Vol. 17, pp. 3-25, (2015).

[36] Mojahedin, A., Farzaneh Joubaneh, E., and Jabbari, M., "Thermal and Mechanical Stability of a Circular Porous Plate with Piezoelectric Actuators", Acta Mecanica, Vol. 83, pp. 57-64, (2014).

[37] Jabbari, M., Mojahedin, A., and Haghi, M., "Buckling Analysis of Thin Circular FG Plates Made of Saturated Porous-softferro Magnetic Materials in Transverse Magnetic Field", Thin-Walled Struct. Vol. 85, pp. 50-56, (2014).

[37] Brush, D.O., and Almroth, B.O., *"Buckling of Bars, Plates and Shells"*, McGraw-Hill, New York, USA, (1975).

[38] Wang, C.M., Reddy, J.N., and Lee, K.H., *"Shear Deformable Beams and Plates: Relationships with Classical Solutions"*, Oxford, Elsevier, (2000).

[39] Detournay, E., and Cheng, A.H.D., *"Fundamentals of Poroelasticity"*, Comprehensive Rock Engineering, Vol. 2, Pergamon Press, New York, USA, (1993).

[40] Eslami, M.R., *"Thermo-Mechanical Buckling of Composite Plates and Shells"*, Amirkabir University Press, Tehran, Iran, (2010).

Nomenclatures

E	: Young's modulus of elasticity
G	: Shear modulus of elasticity
e_1	: Coefficient of plate porosity
ν	: Poisson's ratio
ε_{xx} , ε_{yy}	: Normal strains
γ_{xy} , γ_{yz} , γ_{xz}	: Shear strains
u, v, w	: Displacement components in the x, y, and z directions
u_0 , v_0 , w_0	: Displacement on middle plate surface
p	: Pore fluid pressure
λ_u	: Lame parameters
M	: Biot's modulus
ζ	: Variation of fluid volume content
ν_u	: Undrained Poisson's ratio
B	: Skempton coefficient

α : Biot coefficient of effective stress

ε : Volumetric strain

c_{ij} : Elastic stiffness of the layers

e_{31} , e_{32} : Piezoelectric stiffness

d_{31} , d_{32} : Dielectric constants

E_x, E_y, E_z : Transverse electric field component

V_a : Voltage applied to the actuators in the thickness direction

چکیده

در این تحقیق تحلیل کمانش ورق مستطیلی جامد متشکل از مواد متخلخل با لایه های پیزوالکتریک در شرایط آندرین بررسی شده است. خواص مواد پرو در امتداد ضخامت ورق با تابع مشخصی متغیر می باشد. توزیع تخلخل در امتداد ضخامت ورق به صورت نامتقارن غیر خطی در نظر گرفته شده است. معادلات کلی تعادل مکانیکی غیرخطی و پایداری خطی حاکم بر ورق پرو با لایه های پیزوالکتریک با استفاده از روش حساب تغییرات بدست می آیند. اثرات لایه های پیزوالکتریک بر بار کمانش بحرانی ورق، نسبت ضخامت لایه پیزوالکتریک به پرو و ولتاژ اکچویتور مورد مطالعه قرارگرفته شده است. همچنین تاثیر تراکم پذیری سیال و توزیع تخلخل بر بار کمانش بحرانی در شرایط آندرین ارزیابی شده است. از حلهای تقریبی برای بدست آوردن بار بحرانی کمانش ورق تحت بارگذاری مکانیکی استفاده شده است. نتایج بدست آمده برای ورق های متخلخل با لایه های اکچویتور پیزوالکتریک با داده موجود در تحقیقات پیشین تأیید شده است.